Scientific Research Publishing

International Journal of Geosciences, 2023, 14, 187-208
https://www.scirp.org/journal/ijg
ISSN Online: 2156-8367
ISSN Print: 2156-8359

Mapping and Petro-Structural Study of the Geological Formations of the Alépé Region (South-East of Côte d'Ivoire)

Allialy Marc Ephrem, Diakite Sekou, Houssou N'guessan Nestor, Kouadio Fossou Jean-Luc, Adingra Martial Pohn Koffi

Laboratory of Geology, Mineral and Energy Resources (LGRME), Faculty of Earth Science and Mineral Resources, Félix Houphouët Boigny University, Abidjan, Côte d'Ivoire
Email: allialy@hotmail.fr

How to cite this paper: Ephrem, A.M., Sekou, D., Nestor, H.N., Jean-Luc, K.F. and Koffi, A.M.P. (2023) Mapping and Petro-Structural Study of the Geological Formations of the Alépé Region (South-East of Côte d'Ivoire). *International Journal of Geosciences*, **14**, 187-208.
https://doi.org/10.4236/ijg.2023.142009

Received: December 23, 2022
Accepted: February 6, 2023
Published: February 9, 2023

Abstract

This study focuses on the petrographic and structural characteristics of the geological formations of the Alépé region in the Comoé basin. The petrographic characterization allows us to retain that the study area abounds in a variety of lithologies: amphibole metagranite, metadiorite, amphibolite and metagrauwacke. The lineament map attests that the study area was affected by polyphase tectonics (ductile and brittle), all these deformations have NW-SE to NNW-SSE; NW-ESE to NW-SE; ENE-OSW and NE-SW directions. Coupled geochemical data show that the protoliths of the studied rocks evolve between granites and gabbros that are weakly to moderately be altered. They would originate from continental crust and mantle and would be emplaced in collision contex.

Keywords

Lithostructural, geochemistry, Birimian, Comoe Basin, Alépé, Côte d'Ivoire

1. Introduction

Côte d'Ivoire is geologically based on two major lithological complexes. The Crystalline basement (97.5 %) is characterized by Archean and Paleoproterozoic domains. Sedimentary bassin (2.5%) is represented by oceanic material from Tertiary and Quaternary event. The crystalline basement is divided into two domains separated by the N-S Sassandra fault [1]. The Archean domain, also called the Kenema-Man domain, is located on the west of this fault, while the Lower Proterozoic domain, also called the Baoulé-Mossi domain, is located on

the east of the fault. In order to understand the geology of Côte d'Ivoire, many studies have been conducted, particularly on the Birimian geological terrains that were structured during the Eburnian orogeny [2] and that abound in numerous metalliferous deposits and showings [3] [4] that are being explored or mined. These terrains contain several petrographic facies that are the focus of this study. The Paleoproterozoic age formations in this study are located in southeastern Côte d'Ivoire. However, the Alépé granitoids remain poorly studied, despite their mining potential. In this area, the study conducted by [5] in this region has highlighted several rock types such as metagranitoids (biotite and metamonzogranite); biotite and amphibole fine gneisses; amphibolites as well as the works [6] on the metamorphic evolution in the Comoé Basin and those [7] on the nature of complex tectonic processes as well as the position and origin of the mantle and/or crustal magmas, no detailed geochemical study of the whole igneous complex has been established. Therefore, the objectives of this paper are: 1) to present the petrographic and geochemical characteristics of the Alépé amphibole granites and amphibolites; and 2) to propose a petrogenetic model of the emplacement of these Alépé rocks in the context of the geodynamic evolution of the Birimian sedimentary basin, taking into account previously published works.

2. Study Framework

2.1. Location

Alépé is located in the Mé region, in the south-east of Côte d'Ivoire, 45 km from the economic capital Abidjan, between 5˚10' and 5˚50' North Latitude and 3˚38' and 3˚50' West Longitude. It is bounded by: the villages of Yakassé-Comoé and M'Bon-Houin to the north, the village of Andou M'Batto to the south, the sub-prefecture of Bongo to the east, the villages of Grand-Alépé and Memni to the west (Figure 1).

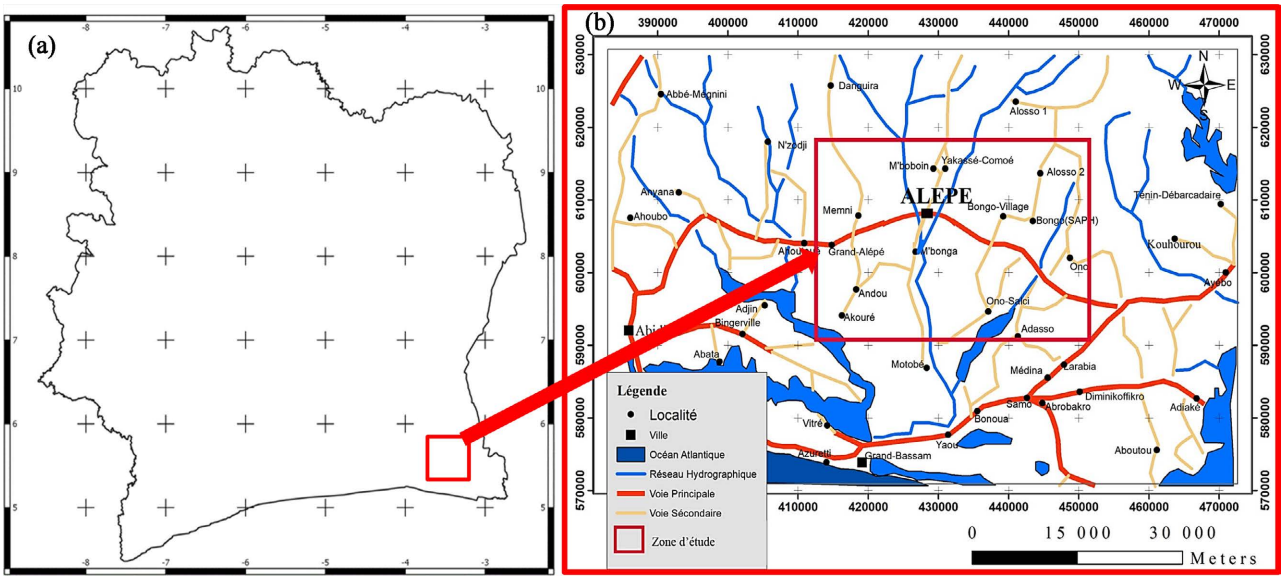

Figure 1. Location map of the study area. (a) Map of Côte d'Ivoire and (b) location of the Alépé region.

2.2. Geological Contex

The West African Craton (WAC) is, according [1], subdivided into three distinct zones (**Figure 2**): To the north, the Reguibat Ridge consisting of Archean formations (3.0 - 2.7 Ga) separated from the Paleoproterozoic formations (~2 Ga) by the Zednes Fault (northern extension of the Sassandra Fault), and outcropping in Algeria, Morocco and Mauritania. To the south, the Man or Leo Ridge formed by the Archean series of the Liberian Shield, and the Paleoproterozoic (Birimian) formations of the Baule-Mossi Domain covering Ghana, Côte d'Ivoire, Guinea, southern Mali, Burkina Faso, and western Niger. The Liberian basement and the Birimian series are separated by an Archean-Proterozoic transition zone [8], corresponding to a large complex fault: the Sassandra submeridian fault [1] [9]. In an intermediate position between the two ridges are two buttonholes, including the Kayes buttonhole in western Mali and the Kenieba-Kedougou buttonhole located on either side of the Senegalese-Malian border. These buttonholes are formed exclusively by Birimian series. The Ivorian Precambrian basement is a characteristic part of the Man Ridge and is essentially composed of a western Archean domain and an eastern Proterozoic domain. The Archean-Proterozoic transition of Cote d'Ivoire, according [1] [9], is materialized by a large complex

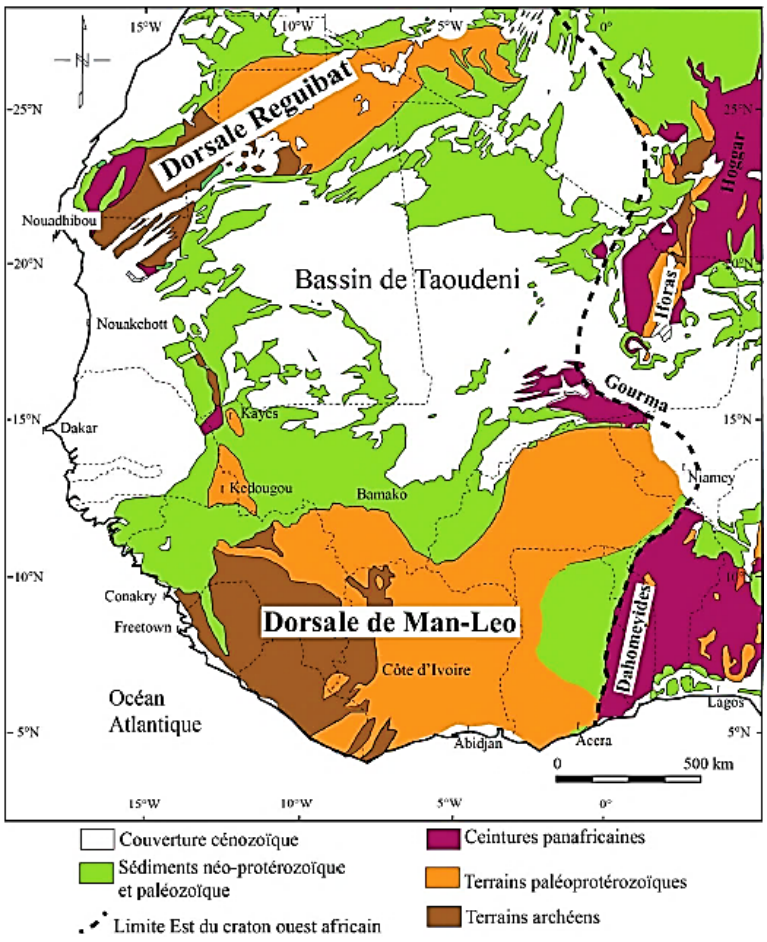

Figure 2. Geologic map of the West African craton (Berger *et al.*, 2013 modified).

fault called the Sassandra Submeridian Fault, with a N-S to NNW-SSE orientation. [10] [11] The study area is located southeast of the Baoulé-Mossi domain, in the Grand-Bassam square degree. The geological formations encountered are essentially composed of late-Eburnian intrusive massifs comprising metagranitoids (metamonzogranite and muscovite metagranite) intruded by tourmaline and beryl pegmatites, Around these metagranitoids are observed metamorphic rocks including biotite and amphibole fine gneisses, amphibolites and amphibolitic gneisses and sedimentary rocks composed of clayey sands of the high plateaus are described (Figure 3).

3. Analytical Methods

Before A geo-traverse of the study area allowed the collection of data, both lithologically and structurally, preceding a number of analytical works in the laboratory. These include macroscopic and microscopic petrography associated with meso- and micro-structural analysis. The thin sections of these rocks were made in the laboratory of Base Geology and Metallogeny of the University Félix HOUPHOUËT BOIGNY-Abidjan. These thin sections were studied under the petrographic microscope to identify the main minerals and the nature of the rock. 10 samples were selected and sent to the VERITAS laboratory for geochemical analysis (Table 1 and Table 2).

4. Results

4.1. Tele-Analytical Data

The processing of the "RADARSAT1 image" of the study area allowed to propose the lineament map of the said area. A total of 275 lineaments were identified.

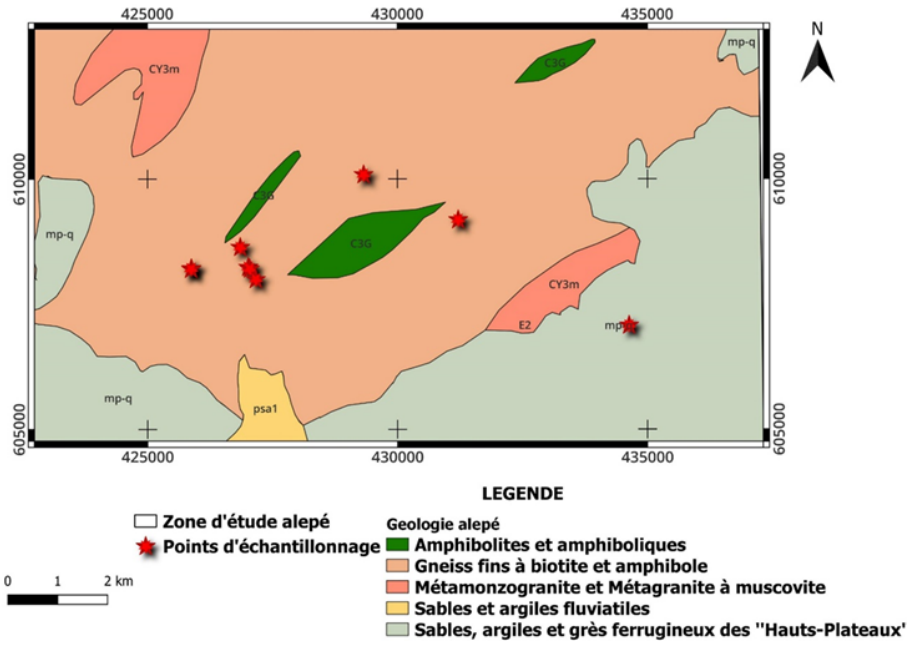

Figure 3. Map of different sampling points location 1/200.000 (Delor *et al.*, 1992 modified).

Table 1. Major elements geochemical patterns of ALEPE amphibolites.

Major elements %	SAMPLE	METAGRANITE					AMPHIBOLITE				
		Alep1	Alep3	Alep6	Alep2	Alep7	Alep4	Alep5	Alep8	Alep9	Alep10
	SiO_2	72.8	71.4	76.4	70.3	78.2	51.84	56.22	49.54	59.49	51.59
	Al_2O_3	14	14.55	10.35	13.7	12.95	15.76	12.05	14.35	15.24	15.4
	Fe_2O_3	1.15	1.1	5.11	3.42	0.61	8.89	14.86	14.7	5.98	10.38
	MnO	0.03	0.01	0.04	0.04	0.01	0.132	0.185	0.242	0.152	0.172
	MgO	0.17	0.17	0.91	1	0.08	5.91	2.77	5.42	2.46	6.56
	CaO	1.35	1.75	0.45	1.73	0.49	11.95	6.875	7.25	3.607	9.788
	Na_2O	5.35	5.69	2.56	3.33	2.04	2.19	2.83	3.66	3.37	3.37
	K_2O	2.92	2.48	1.28	2.26	0.5	0.219	0.545	0.576	2.591	0.271
	TiO_2	0.09	0.1	0.57	0.31	0.42	0.554	2.163	1.803	0.783	0.975
	P_2O_5	0.01	0.05	0.06	0.06	0.03	0.091	0.369	0.211	0.158	0.097
	Cr_2O_3	0.01	0.01	0.01	<0.01	0.01	0.01	0.01	0.01	<0.01	0.01
	SrO	0.06	0.07	0.02	0.01	0.03	0.06	0.07	0.02	0.01	0.03
	BaO	0.07	0.07	0.04	0.03	0.07	0.07	0.07	0.04	0.03	0.07
	LOI	0.86	0.61	1.78	3.11	4.04	1.98	0.58	1.65	5.24	0.85
	Total	98.86	98.04	99.58	99.3	99.47	99.63	99.63	99.65	99.48	99.5

Table 2. Composition of traces elements (REE) in studies rocks.

	SAMPLE	METAGRANITE					AMPHIBOLITE				
		Alep1	Alep3	Alep6	Alep2	Alep7	Alep4	Alep5	Alep8	Alep9	Alep10
Traces elements (ppm)	As	0.2	1.1	1	9.2	2.3	5	3	3	6	5
	Au	686	1050	1015	0.02	0.01					
	Ba	<0.01	<0.01	0.05	274	595	68	208	132	899	106
	Bi	0.03	0.16	0.01	0.03	1.28	2.4	2.5	2.7	2.3	2.9
	C	0.02	0.16	0.08	0.4	1.77					
	Co						31	42	36	18	39
	Cr	30	40	30	30	40					
	Cs	1.62	5.01	2.31	1.69	1.74	10	11	10	11	4.5
	Cu						8	20	44	32	29
	Ga	22.7	18.7	16.5	16	19.5	18	18	21	18	18
	Hf	3.3	4.9	4.2	3.7	3.3	4	3	4	3	2
	Hg	<0.005	0.01	0.01	0.13	0.01					

Continued

Mo						2	1.5	2	3	1.7
Nb	4.4	11.7	6.7	7.3	8.4	1.8	13	6	9	1.5
Ni						55	2.7	55	26	40
Pb						3	2	3	2	3
Rb	49.5	106	102	71.3	16.5	5	15	17	80	8
S	<0.01	0.05	0.01	<0.01	0.01					
Sb	0.04	0.05	0.07	0.25	0.73	4.6	7	4.8	4.5	4.7
Se	0.4	0.3	0.2	0.2	0.2	31	32	41	14	37
Sm	3.93	5.38	4.5	2.77	4.35					
Sn	<1	2	1	2	3	1.5	1.1	1.6	1.7	1.8
Sr	871	311	414	45.5	262	265	138	154	529	230
Ta	0.3	0.9	0.5	0.8	0.7	4	2.9	4.6	4.7	4.1
Tb	0.32	0.52	0.41	0.37	0.47					
Te	<0.01	0.01	0.01	0.05	0.9					
Th	2.36	11.7	7.51	4.62	5.25	3	8	7	8	7
Tl	0.5	<0.5	0.5	<0.5	0.5					
Tm	0.17	0.11	0.16	0.22	0.19					
U	0.49	2.06	1.41	1.6	3.22	2	4	2.5	5	2.7
V	58	69	55	48	227	203	353	360	87	212
W	<1	1	1	4	3	4.9	4.1	4.7	4.3	4.5
Y	7.2	13.6	11.7	14.3	12.4	14	36	33	20	26
Zn						54	134	105	62	74
Zr	130	200	160	160	130	47	199	101	179	71
La	24.6	57.8	37.9	20	28.9	13.5	12.3	37.2	6.3	5
Ce	49.5	107.5	73.1	37	53.3	28.4	25.7	74.5	11	12
Pr	5.96	11.35	8.42	3.89	6.26	3.89	3.36	9.35	1.9	1.81
Nd	24.1	37.4	29.1	14	23.1	16.1	13.9	35.9	9.8	8.7
Sm	3.93	5.38	4.5	2.77	4.35	3.82	3.24	6.4	2.69	2.44
Eu	1.16	1.24	1.15	0.76	1.02	1.08	0.94	1.77	0.99	0.89
Gd	2.65	3.83	3.15	2.4	3.36	3.75	3.1	4.54	3.73	3.12
Tb	0.32	0.52	0.41	0.37	0.47	0.57	0.49	0.55	0.67	0.58
Dy	1.43	2.59	2.15	2.19	2.39	3.13	2.8	2.71	4.21	3.58
Ho	0.26	0.49	0.42	0.45	0.49	0.63	0.58	0.51	0.93	0.82

Continued

	Er	0.69	1.27	1.13	1.32	1.3	1.71	1.55	1.28	2.76	2.37
	Tm	0.17	0.11	0.16	0.22	0.19	0.25	0.22	0.18	0.39	0.32
	Yb	0.59	1.14	1.15	1.31	1.35	1.56	1.44	1.12	2.52	2.15
	Lu	0.08	0.19	0.19	0.21	0.18	0.25	0.23	0.18	0.39	0.35

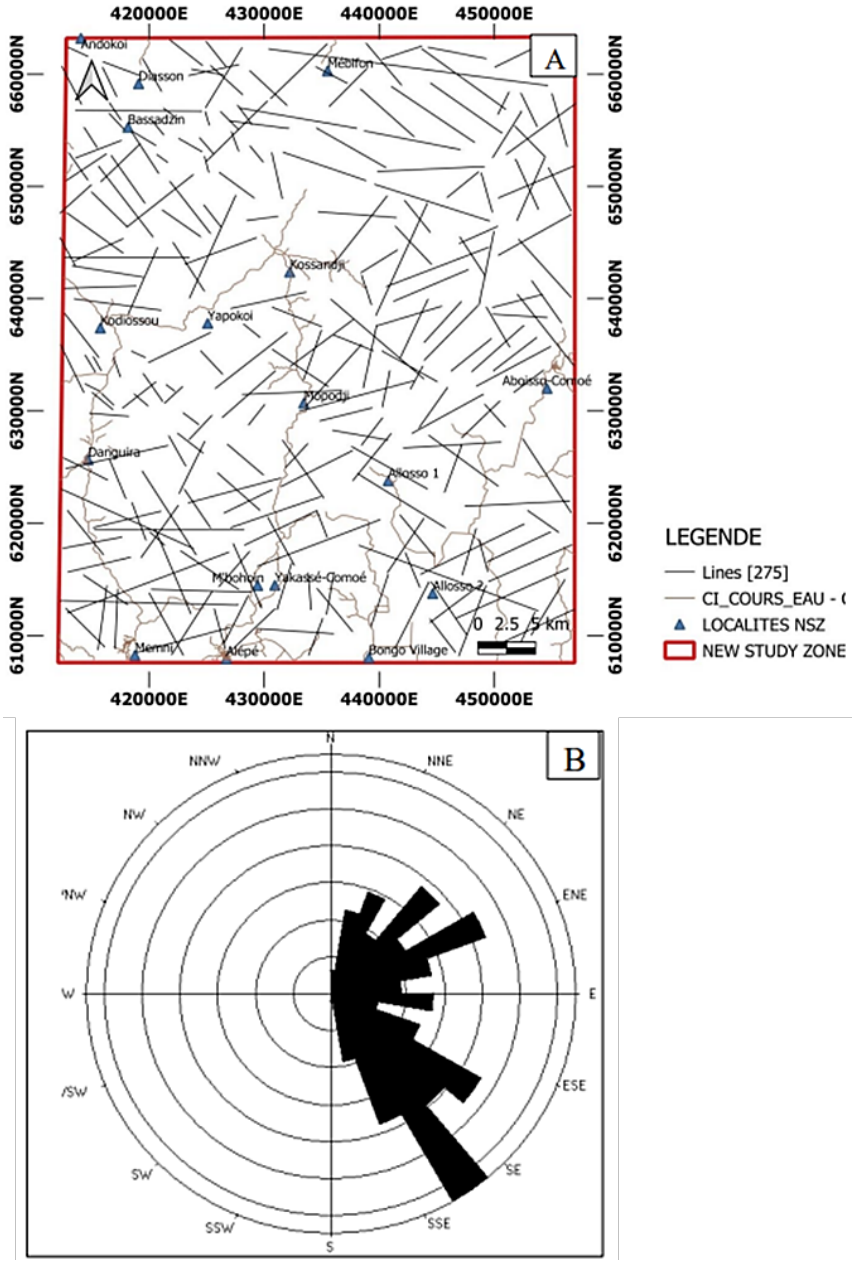

Figure 4. Thematic map of the lineament network (a) of the study area and associated directional rosettes (b) 275 lineaments.

These lineaments have various orientations and lengths (**Figure 4(a)**). The analysis of these directions with the Georient software allowed to highlight the dif-

ferent directions of the lineaments. Four preferential directions emerge, which are: NW-SE to NNW-SSE; NW-ESE to NW-SE; ENE-OSW and NE-SW (Figure 4(b)). These lineaments correspond in the field to fractures, schistosities, veins and seams.

4.2. Petrographic Data

In the following lithological description, the prefix "meta" is intended to be synonymous with the deformed character of the rock considered.

- **Amphibole metragranite**

Amphibole metagranite is one of the major lithologies of the Alépé sector. It is a massive rock that outcrops on certain sites in the form of an accumulation of large balls released by erosion (granitic chaos). The amphibole metagranite observed is generally leucocratic, medium-grained and coarse-grained (Figure 5(a) and Figure 5(b)). At outcrop, these are mostly oriented, slightly to strongly deformed and altered rocks. Due to hydrothermal alteration and deformation, their minerals have been generally modified, giving way to secondary minerals (chlorite, epidote, sericite). We observe a mineral lineation affecting these formations. They are essentially composed of quartz, plagioclase, biotite and amphiboles of variable proportions.

Microscopically, the rock has a gritty to gritty porphyroid oriented texture:

- Quartz: very abundant mineral, xenomorphic, it is variable in size from small crystals to large crystals and presents a remarkable rolling extinction in polarized light (Figure 5(c)).

- Plagioclase: it constitutes with quartz, the minerals most met in the thin slides, in the form of large plates, generally subautomorphic, it is easily identifiable with the polysynthetic macle. Plagioclases are generally phenocrysts, most often altered to sericite (Figure 5(c)).

- Green hornblende: abundant, in large subautomorphic crystals, with two cleavages in basal section and one cleavage in longitudinal section, some shows alteration to chlorite and epidote (Figure 5(f)).

- Biotite: long subautomorphic flakes, brown, with intense direct pleochroism, perfect cleavage in longitudinal section, but grouped and elongated in thin sheets. It presents an arrangement in mineral beds and oriented parallel to these beds (foliation). Zircon inclusions were also observed, with alteration of biotite to chlorite (Figure 5(d)).

- Microcline: in the form of a large beach with irregular contours (xenomorphic), it is scarce in the rock and can be seen through the squared-off macle, which totally disappears four times per complete turn of the platinum. Colorless, it has a gray polarization hue of the 1st order (Figure 5(e)).

As accessory minerals chlorite, epidote, sericite and opaque minerals are also present (Figure 5(c) and Figure 5(f)).

- **Amphibolite**

The amphibolite outcrops as a block, greenish-gray in color. Finely banded, the rock shows alternating light beds of quartz and feldspar minerals, while the

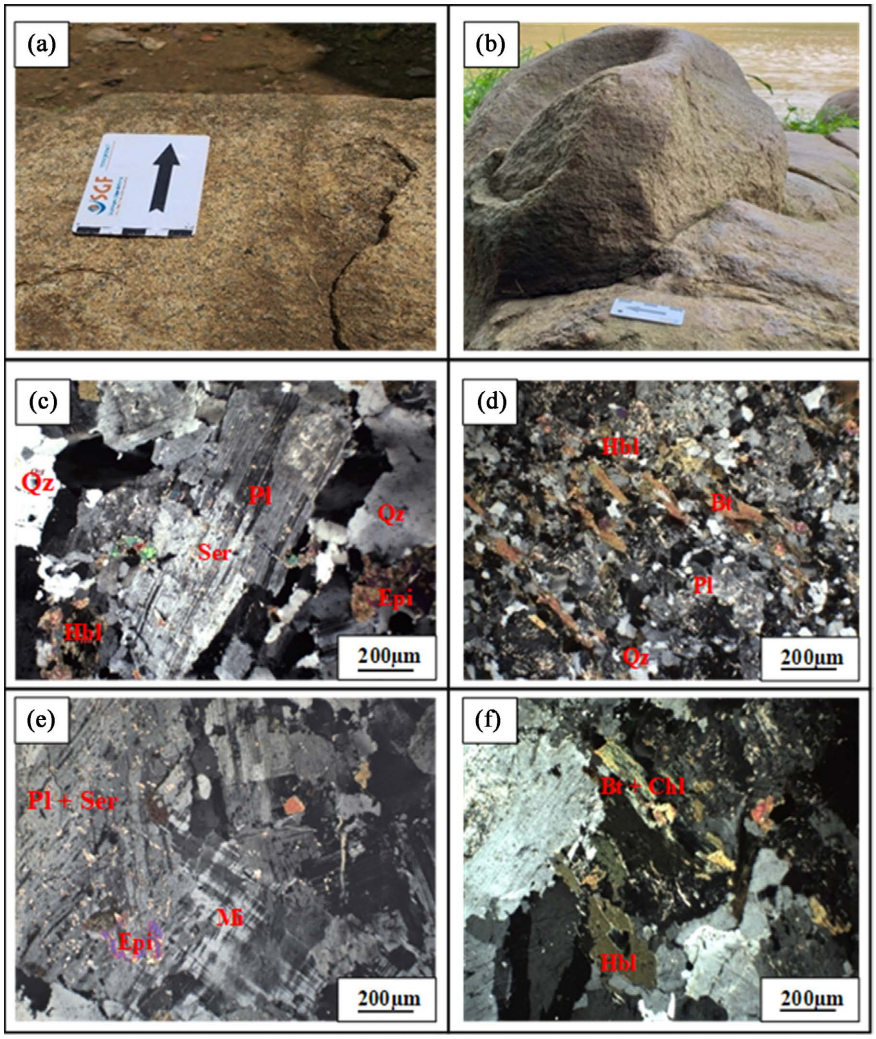

Figure 5. Macroscopic and microscopic aspects of amphibole metagranite. (a) and (b): Macroscopic aspect; (c)-(f): Microscopic aspect. Qz: quartz. Pl: plagioclase. Bt: biotite. Hbl: hornblende. Ser: sericite. Epi: epidote. Chl: chlorite. Op: opaque.

dark or ferromagnesian level shows amphibole enrichment (foliation) (**Figure 6(a)**). Microscopically, the rock has a granitic texture, with the following minerals:

- Green hornblende: very abundant and generally elongated in the form of a needle in longitudinal section, it presents some basal sections. It is pleochroic, from slightly dark green to very light green or even colorless, with bright polarization tints in the yellow to orange yellow of the second order. The mineral is altered, with inclusions of opaque minerals and epidote (**Figure 6(b)**).

- Plagioclase: plagioclase occurs as ghosts, is subautomorphic, colorless and little altered (**Figure 6(d)**).

- Quartz: not very abundant, homogeneously distributed throughout the rock, it is generally oriented in section with a characteristic rolling extinction, indicating the deformation of the rock. It polarizes in the light gray of the end of the first order (**Figure 6(d)**).

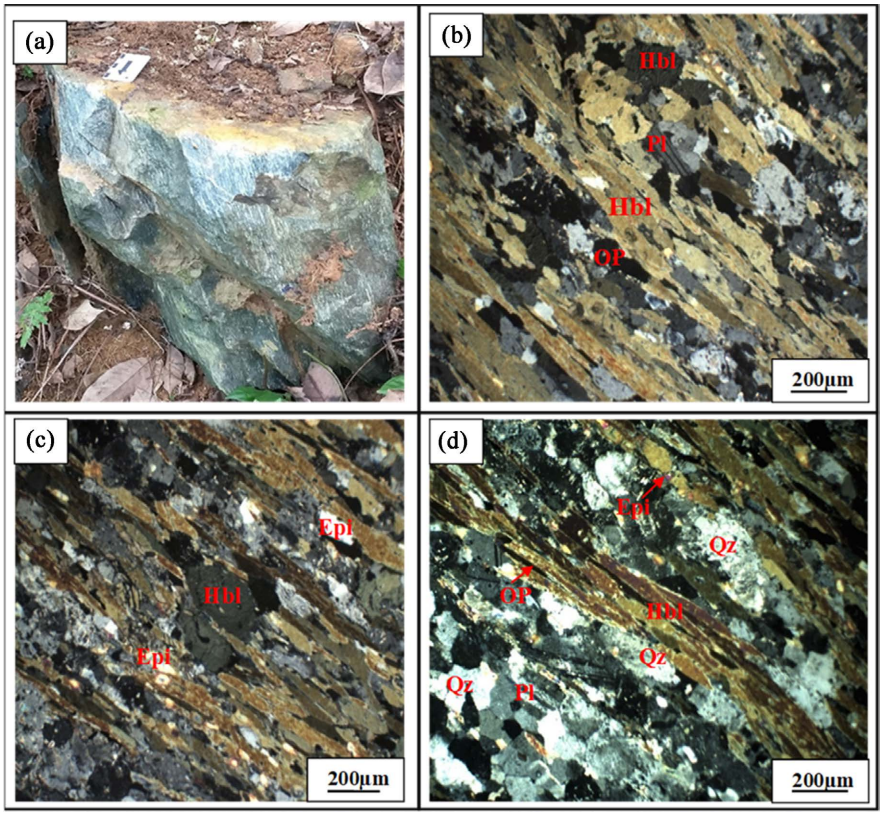

Figure 6. Macroscopic and microscopic aspects of the amphibolite. (a) Macroscopic aspect; (b)-(d) Microscopic aspect. Qz: quartz. Pl: plagioclase. Hbl: horn-blende. Epi: epidote. Op: opaque.

- Epidote: resulting from the destabilization of amphibole in the form of small crystals, it is xenomorphic, of the millimeter order, colorless to yellowish and polarizes in the purplish blue to yellowish identical to the harlequin coat (**Figure 6(c)**).

4.3. Structural Data

- **Ductile deformations**

Foliation in amphibolite. It appears as alternating dark and light bands, marked by the ferromagnesian and quartzo-feldspathic minerals that make up the rock. These bands are visible in the horizontal and vertical planes (**Figure 7(a)**). This foliation thus characterizes the tectonic "S". The foliation in the amphibolite has a N 150˚ direction with a dip of 75˚ to the SW.

The fold observed at Alépé corresponds to a folded quartz vein (**Figure 7(b)**). It is indeed a driving fold with a fold axis parallel to the foliation oriented N120˚. This fold has an M-shaped structure observed at the hinge and a Z- and S-shaped structure observed at the flanks. The linear fabric observed in the Alépé sector is poorly represented and is expressed subhorizontally or subvertically (**Figure 7(c)**). A subhorizontal lineation oriented N 0-2˚. However, at the level of some oriented amphibole metagranites, the mineral stretching lineations are very well marked, oriented N90˚ and plunging 70˚W.

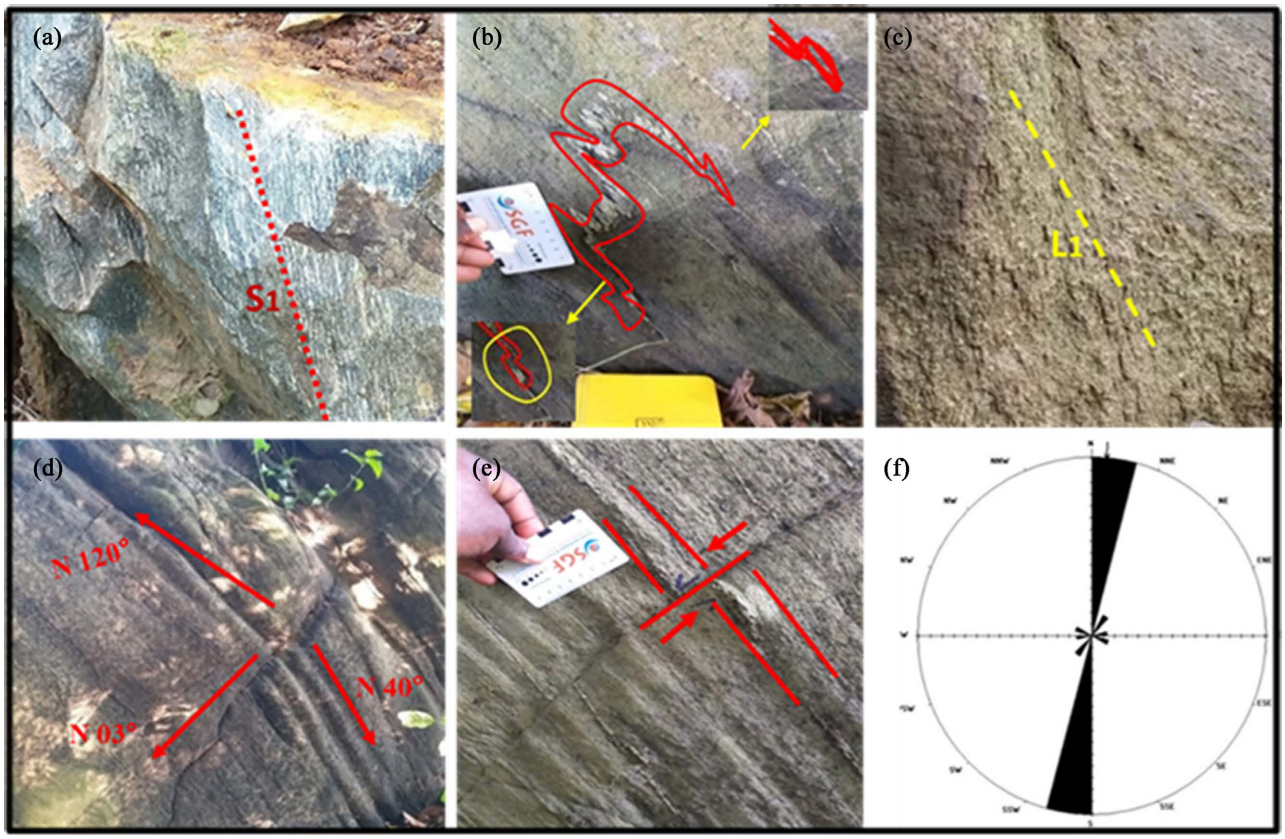

Figure 7. (a) Foliation in the amphibolite. (b) M-hinged, Z- and S-flanked entrainment fold marking dextral shear. (c) Subvertical mineral stretching lineation observed in the amphibole metagranite. (d) Fracture set. (e) Sinister break-up. (f) Directional rosette of the veins.

- **Microstructural analysis and metamorphic evolution**

The microstructural approach allowed to highlight two (2) phases of deformation at the interface of three successive generations of minerals (**Figure 8(a)**). The first generation of minerals is composed of large quartz marked by a characteristic undulating extinction, in this generation, a phase of biotite characterized by rods showing an orientation. The deformation that affected the primary minerals is accompanied by a mineral recrystallization forming the second generation that surrounds the quartz phenoblasts. This generation of minerals is composed of quartz of smaller size and oriented. One notes, always in this generation, the oriented brown biotite. The third generation of minerals also appears by neoformation following a probable alteration. It is sericite in plagioclase. The rock shows numerous fractures in which a secondary association with Qz-Ep develops (**Figure 8(b)**). The presence of quartz veinlets and epidote veinlets in the thin sheet allows us to assert that these fractures were accompanied by hydrothermalism. These different observations allow us to consider a syn to late-tectonic emplacement of the amphibole metagranite. Some of the minerals observed have mineralogical assemblages consisting of chlorite, epidote and sericite, minerals characteristic of greenschist metamorphic facies. These symptomatic minerals characterize low temperature (epizone) and low pressure conditions,

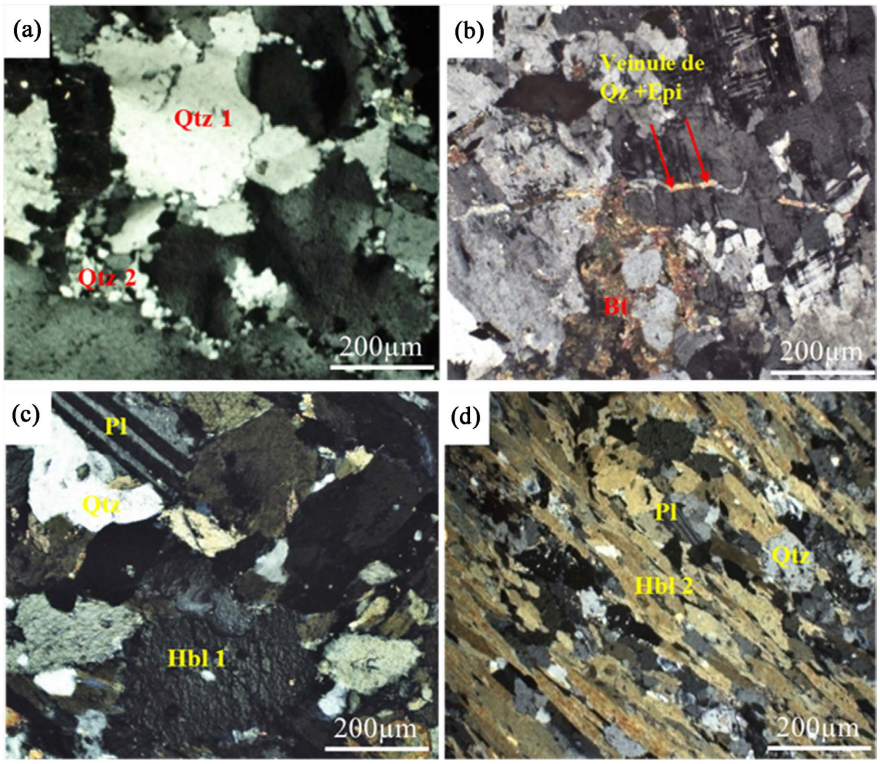

Figure 8. (a) Quartz subgrain showing dynamic recrystallization, (b) Illustration of quartz veinlets and secondary minerals following shearing of the amphibole metagranite (c) and (d): Overlay of ferromagnesian on felsic rocks.

typical of greenschist facies.

The amphibolite sample taken in the Alépé sector revealed a mineralogical assemblage composed of hornblende + quartz + opaque minerals (**Figure 8(c)** and **Figure 8(d)**). As for the microstructural analysis, it revealed two (2) generations of minerals. Antecinematic minerals observed are pseudomorphosed hornblende. The secondary minerals characterized by an orientation parallel to the foliation are hornblende and quartz. The paragenesis thus formed is characteristic of a metamorphism of medium degree, typical of the amphibolite facies.

4.4. Geochemical Data

4.4.1. Characterization and Classification

The chemical compositions of samples from the different formations are projected into the different rock classification digrams for characterization. Inserted in the $Na_2O + K_2O$ (wt%) versus SiO_2 (wt%) diagram [12], the granitoids show predominantly granitic compositions (amphibole metagranite). These results appear consistent with field petrographic data. In the R1 vs R2 space according [13], calculated on the basis of the proportions of the elements in millication, the granitoids studied range from the granite domain to the granodiorite domain. Projected in the A/CNK VS A/NK diagram, the granitoids of the study area show mostly peraluminous to weakly metaluminous characters. In the K_2O vs. SiO_2 diagram [14], all granitoids show calc-alkaline to moderately tholeitic affinities

(**Figure 9(a)**).

Inserted into the $Na_2O + K_2O$ (wt%) versus SiO_2 (wt%) diagram [12], the basic volcanics (amphibolite) show basaltic and andesitic trends. The proportion of elements in millications calculated in basic volcanics in the diagram [13], ranges from the basalt domain through the dacite domain to the andesite domain and shows tholeiitic to low-K calc-alkaline and high-K calc-alkaline affinities in the AFM diagram [15]. In the A/CNK VS A/NK diagram [16] the amphibolites of the study area show predominantly metaluminous to weakly peraluminous characters (**Figure 9(b)**).

4.4.2. Geochemical Evolution

The SiO_2 vs. Harker Oxides diagrams show a clustered and linear distribution of points representative of granitic (amphibole metagranite), basaltic (amphibolite) rock samples in the study area. This distribution indicates positive correlations between SiO_2 and the majority of elements, notably P_2O_5, K_2O, Al_2O_3, CaO for the samples with granitic composition (amphibole metagranite) and much less with NaO_2, FeOt, MgO. A positive correlation exists between SiO_2 and the elements CaO, MgO, Al_2O_3 for samples with basic composition (amphibolite). In detail, the granitic and basic formations of the Alépé area show a continuity of composition (**Figure 10**).

4.4.3. Petrogenetic Signatures

The rare earth element (REE) spectra of the different formations are almost similar; they are characterized by more or less fractionation between light rare earths (LREE) and rare earths (**Figure 11**).

(a): The rare earth content (∑REE) of the amphibole metagranite is 163.82 ppm and 230.29 ppm. The amphibole metagranite samples show moderate fractionation of the LREE rare-earth spectra [(La/Yb)N = 16.89 and 84.91], slight negative Eu anomalies (Eu/Eu* = 0.71 to 0.96) due to plagioclase fractionation, and subflat HREE spectra (**Figure 11(a)**).

In normalized multi-element diagrams at the early mantle, the majority of rocks show enrichment in Large Ion Lithophile Elements LILE (e.g., Cs, Th, k, U) and depletion in Ba, Rb, Sr, Eu, Nb, and high-field electrostatic elements (HFSEs) (e.g., Zr, and Ti) rela-tive to the rare-earth elements, expressed as positive and negative anomalies, respec-tively (**Figure 11(a)**). The pronounced negative Ba anomaly observed in the amphibole metagranite is due respectively to the development of secondary muscovite during hydrothermal alteration and to the destabilization of feldspars. Chemical data, projected in the Rb versus Y+ Nb binary dia-grams of Pearce *et al.* (1984), provide information on the petrogenetic and geotectonic relationships of granitoids (**Figure 11(a)**). Because of their low Ta, Y, and Nb contents, almost all granitoids fall in the volcanic arc granite (VAG) fields.

(b): The rare earth content (∑REE) of the amphibolites is 78.64 ppm and 176.19 ppm. The amphibolite sample shows a moderate LREE fractionation ([La/Yb]N) that does not exceed 2.32 and a slightly negative Eu anomaly

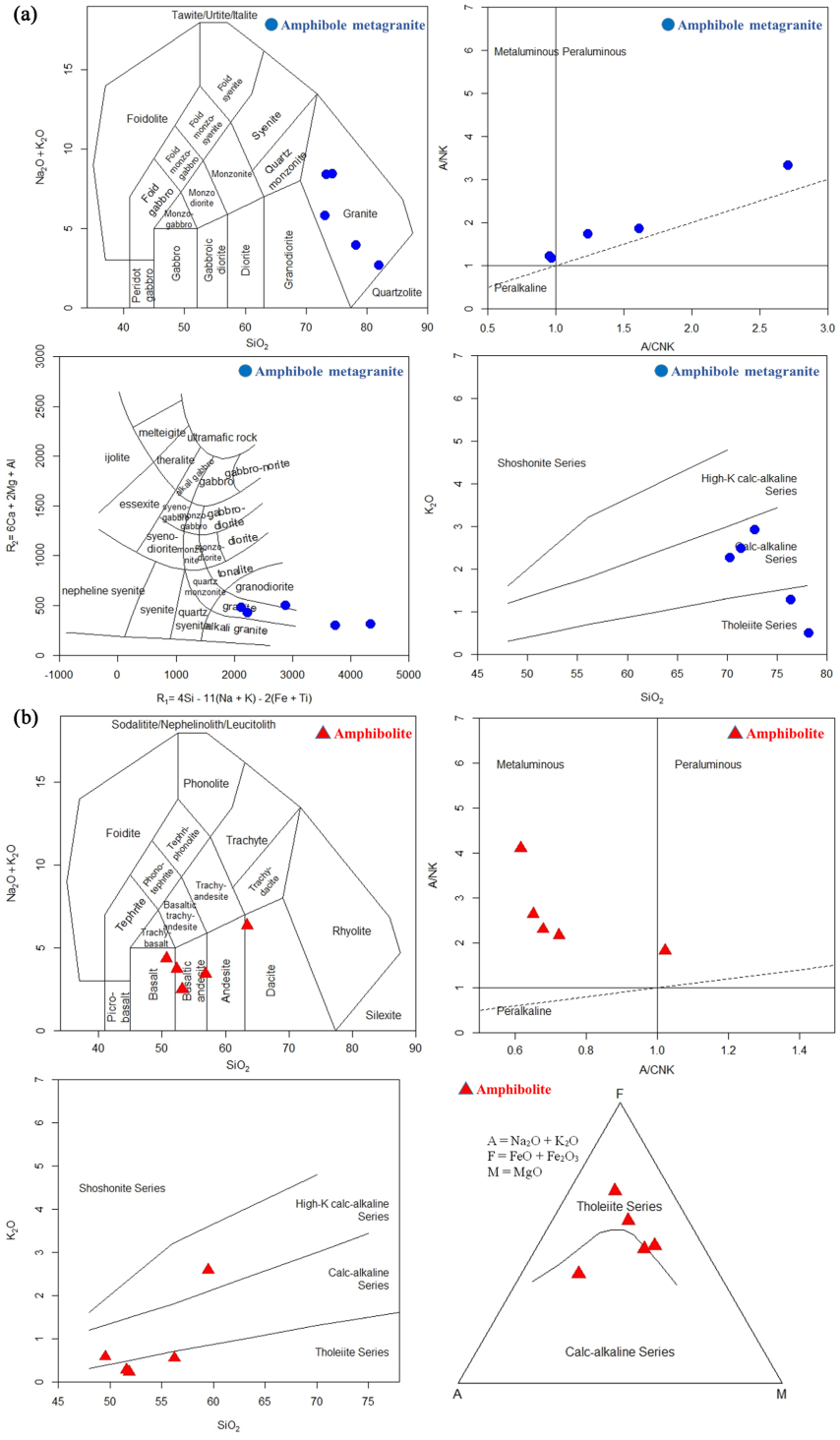

Figure 9. Classification diagrams of the different formations of the Alépé area. (a) Amphibole metagranite) and (b) Amphibolite): diagram $Na_2O + K_2O$ according to SiO_2 of Middlemost (1994) of plutonites and volcanites. (a) Amphibole metagranite) and (b: Amphibolite): classification using R1 and R2 parame-ters (after De la Roche *et al.*, 1980), calculated on the basis of the proportions of elements in millication. (a) Amphibole metagranite) and (b: Amphibolite): A/NK vs A/CNK diagram after Shand (1934). (a) Amphibole metagranite): K_2O vs. SiO_2 diagram from Peccerillo and Taylor (1976); (b) Amphibolite): AFM diagram of Irvine and Baragar (1971).

(Eu/Eu* = 1.54 - 1.65). The latter is due to plagioclase fractionation and shows almost identical spectra in the HREE part (Figure 11(b)).

The multi-element spectra normalized to the early mantle, the majority of the rocks show enrichment in Large Ion Lithophile Elements LILE (e.g. Cs, Th, U, pb) and depletion in Ba, Rb, Sr, K and High Field Electrostatic Elements (HFSE) (e.g. Zr) with respect to the rare earth elements, expressed by positive and negative anomalies respectively (Figure 11(b)).

Data from the basic volcanic rocks are projected in the Zr vs. Zr/Y diagram of Pearce and Norry (1979), indicates that the amphibolites are in the MORB-CAB-

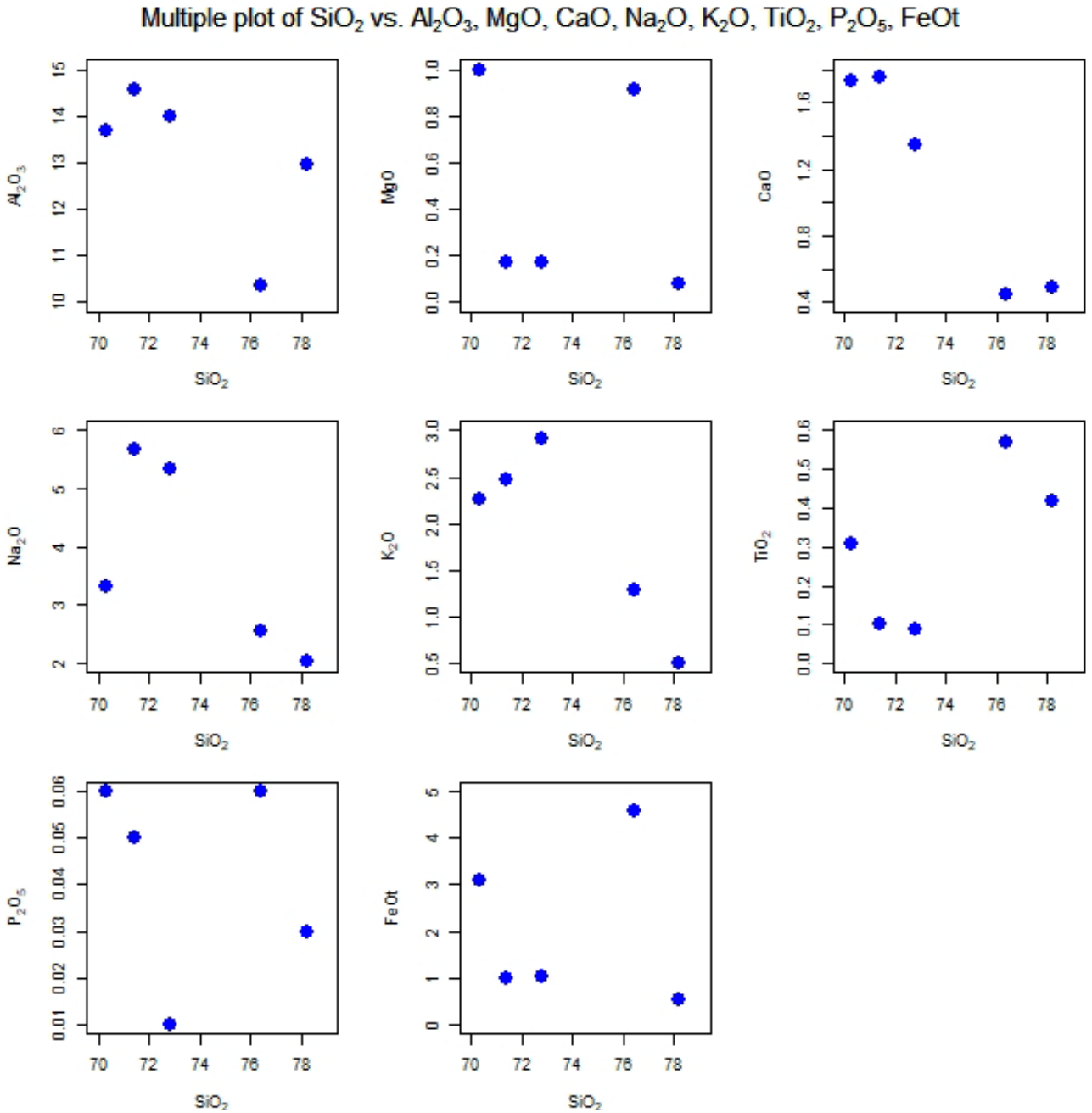

(a)

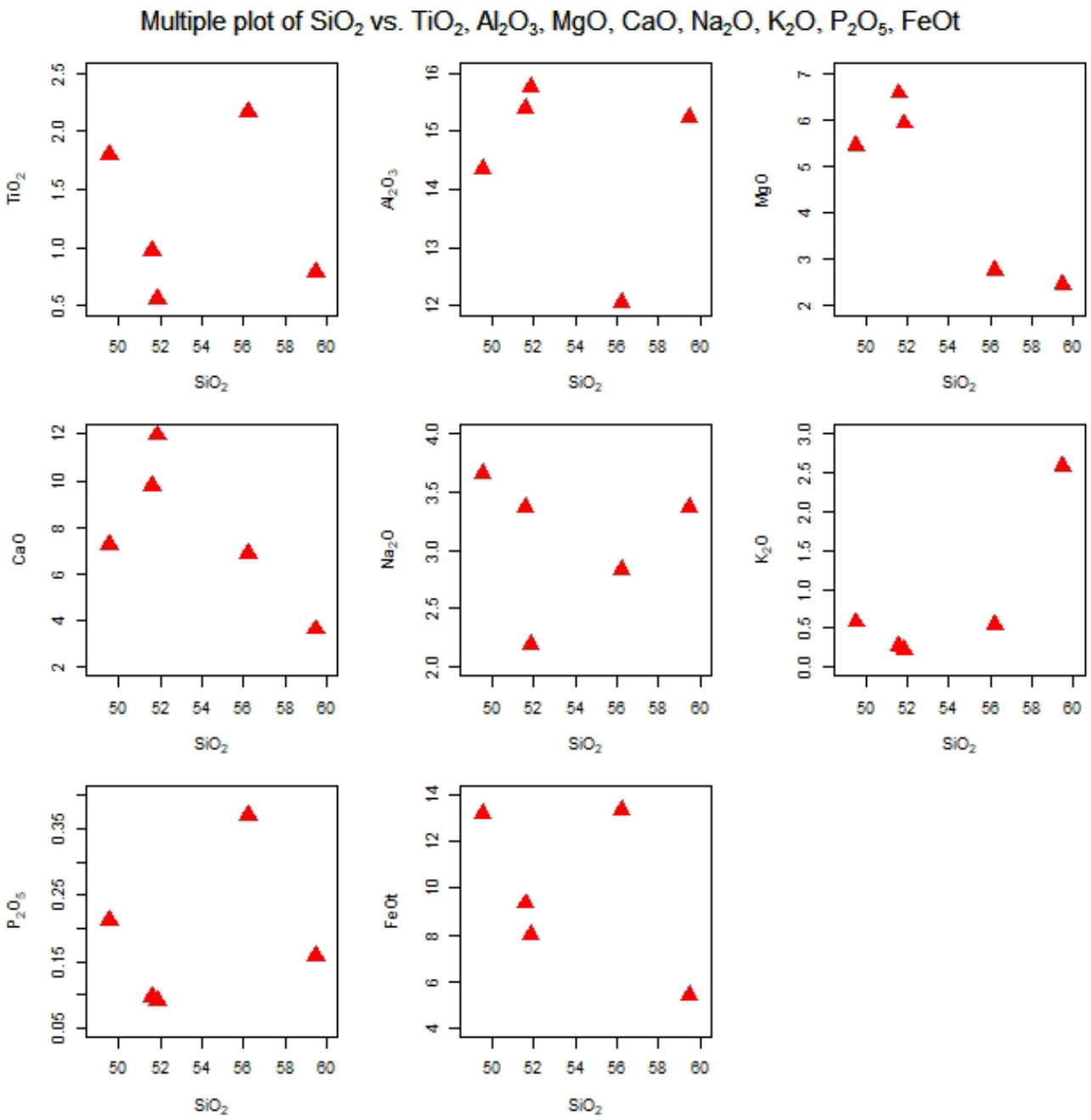

(b)

Figure 10. (a) Amphibole metagranite) and (b) Amphibolite) distribution of the formations in the study area (Alépé) in the Oxides vs SiO2 Harker diagrams.

IAT field and confirms that these amphibolites have a tholeiitic affinity and are derived from arc magma (**Figure 11(b)**).

4.4.4. Geodynamic Evolutionary Contex

The opening of the Comoé basin occurred in an extensive NW-SE context [17]. Significant enrichments in LILE and pronounced Nb-Ta anomalies reflect a subduction environment (Hoffer, 2008). Indeed, TiO2 levels below 2% suggest

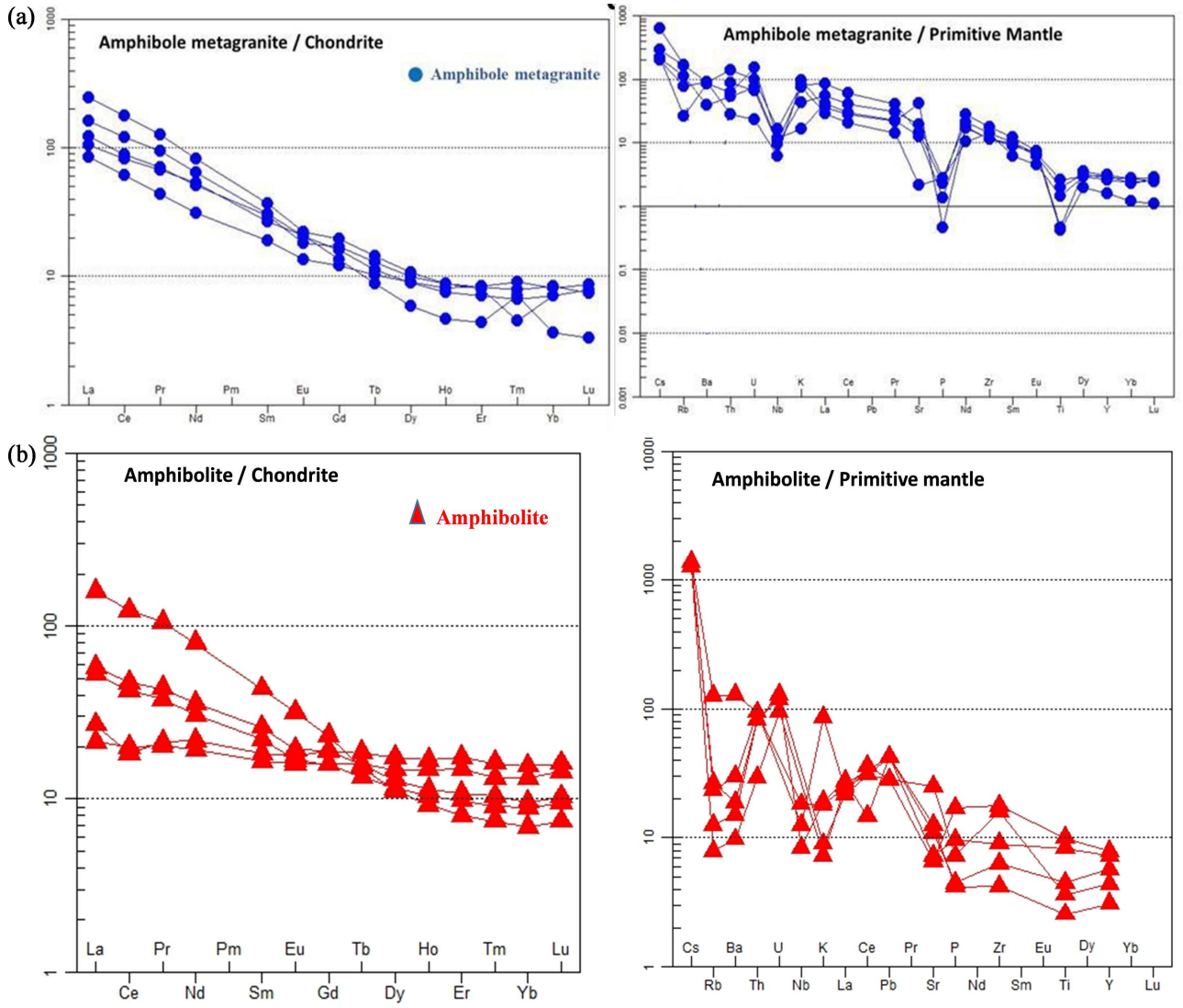

Figure 11. Rare-earth spectra normalized to chondrites (after Anders & Grevesse, 1989) and trace-element spectra normalized to the primitive mantle (after Sun & McDonough, 1989) of samples ((a) Amphibole metagranite and (b) Amphibolite) from Alépé.

emplacement in a volcanic arc context, responsible for the emplacement of volcanites and granitoids from volcanic and collisional arcs. The presence of sediment deposits is due to the alteration of greenstone and granitoids in the basin. The compressional tightening of the basins (phase D1) E-W to WNW-ESE, results in the formation of S1 schistosity. It is accompanied by a thickening of the crust and the setting up of syntectonic plutons.

The associated magmatism is essentially calc-alkaline and is linked to plunging plates [18]. The episode of ductile deformation is related to the D2 phase, set up during the NW-SE transpressional phase. It develops a S2 schistosity, strongly penetrating in the form of flow. A subvertical stretching lineation is associated with this phase. The shortening of the volcanic arcs is accompanied by the emplacement of plutons that may have originated from the lower mafic crust (Figure 12).

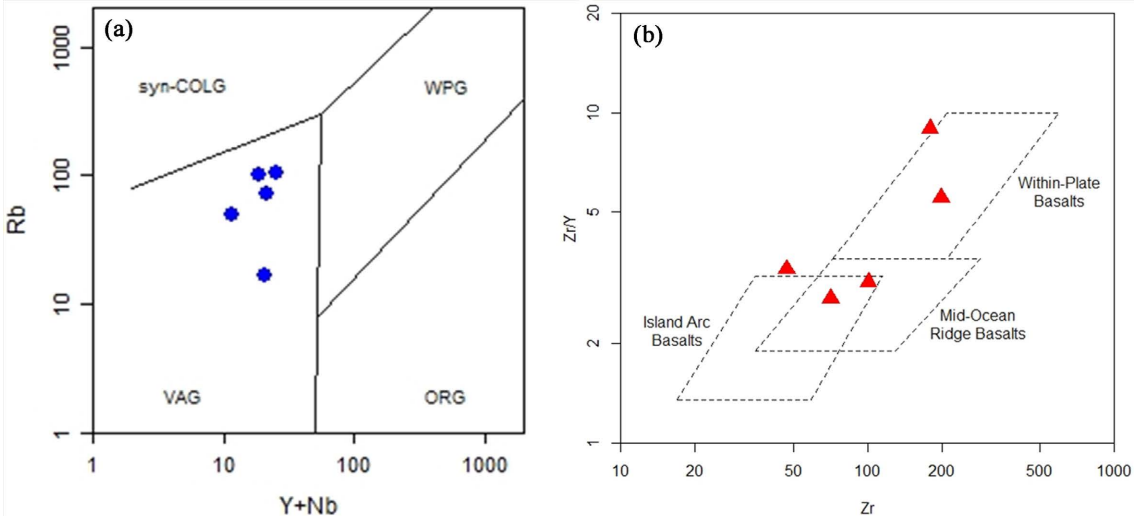

Figure 12. (a) Amphibole metagranite)**:** Rb vs Y+ Nb binary diagram from Pearce *et al* (1984); (b) Amphibolite): Zr vs Zr/Y diagram of Pearce and Norry (1979).

5. Discussion

5.1. Petrology

The study area contains several lithologies. It is essentially composed of amphibole metagranite, metadiorite, amphibolite and metagrauwacke. The work [5] [19] have highlighted these same formations. According to these authors, the amphibole metagranite and the metadiorite are late-Eburnian intrusive masses. These are consistent with the work [20]. In his report on the granites of southeastern Cote d'Ivoire, he individualizes syntectonic, late-tectonic and post-tectonic plutons within the Birimian metamorphic series. These same facies have been reported by the work [21] in the Comoé unit with similar mineralogical compositions. Concerning the genesis of the Eburnian granites, [22] contrasts a calc-alkaline series whose granodioritic precursors are thought to be around 2000 ± 50 Ma with a more recent alkaline series (2050 - 1900 Ma. The amphibolite, based on its mineralogical composition and its spatial arrangement (amphibolite-gneiss alternation), would derive from a magmatic origin. These are ortho-amphibolites; this has been highlighted in the Divo, Oumé and Taabo regions and these rocks constitute the most widespread Birimian greenstone facies [23] [24]. In addition, the work of Tagini [19] [25] in the Comoé unit showed that the Eburnian metamorphosed formations in the greenschist facies are underlain by a granitogneissic basement.

5.2. Tectonic

All of these deformations highlighted in our study area confirm the existence of the first and second major deformation phases recognized in the Baule-Mossi domain. In addition, field measurements have established two general structural directions. These are the NNE-SSW and NE-SW directions. These different structures have main directions that follow those of the entire Birimian (NE-SW

to NNE-SSW). Indeed, according [26], the D1 phase is associated with the S1 foliation and the L1 subvertical lineation. Then comes the D2 phase which is a progressive deformation composed of NW-SE bending episodes. It generalizes to give a pure shear in the same direction, which in turn intensifies to give a simple sinister shear oriented N-S to NE-SW. This simple shear is followed by a sinister N03˚ brittle shear. The D2 phase is also responsible for the structuring of the NNE-SSW to ENE-WSW oriented Birimian series. This corroborates the work [27] who confirm the presence of an early regional S1 schistosity that they attribute to the early emplacement of granitic blocks and demonstrate at all scales the senestial shearing character of a regional S2 schistosity.

The microstructural study allowed us to follow the metamorphic evolution and to specify the existence of a prograde metamorphism going from greenschist facies to amphibolite facies. We note in these thin sections, different types of reaction texture: dynamic recrystallizations of quartz with formation of secondary minerals. The formations of this site are constituted of minerals such as green hornblende, brown biotite, plagioclase, quartz, orthose, microcline, muscovite, epidote, sericite and chlorite. The mineralogical assemblage thus described characterizes the amphibolite facies, thus an epizonal to mesozonal metamorphism. This is consistent with the work [1], in the Alépé-Bianouan granite axis.

5.3. Geochemistry

Most of the study area consists of various varieties of formations as revealed by petrographic observations. These include biotite metagranite, metadiorite, amphibolite, metagrauwaycke. The granitoids, show chemical compositions practically similar to those from other birimic domains in general, and in particular those of Dabakala [28] [29].

The peraluminous to metaluminous character suggests that the magmas that generated the rocks are relatively hybrid and derived partly from crustal sources. This confirms the hypothesis of magmatic mixtures, originating on the one hand from the melting of the mantle and on the other hand from the melting of crystalline rocks of the continental crust. The slightly negative Eu anomaly observed in the majority of the magmatic formations of Aleppo ($Eu/Eu^* = 0.71$ to 0.96 for amphibole metagranites and $Eu/Eu^* = 1.54 - 1.65$ for amphibolites) indicates that plagioclase fractionation is important in the evolution of these magmatic formations Moreover, the negative cerium anomaly observed on the different spectra is common to modern arc magmas but may also result from post-magmatic alteration, such as pervasive circulation of hydrothermal fluids [30].

The granitoids would have a hybrid origin (mantle and crustal) because of their calc-alkaline and metaluminous character. The spectra reveal an enrichment in the most incompatible elements (Cs, K, U) with negative anomalies in Sr, Nb which are two characteristic features of magmas of orogenic zones and of the continental crust in general [31].

The amphibolites studied have a sub-alkaline character, the low TiO_2 contents of these volcanics are typical of magmatic arc rocks [32], with a (La/Yb)N ratio not exceeding 2.32 also typical of island arc tholeites [33]. The negative Nb anomalies revealed not only attest to a subduction environment, but also to the fact that their composition varies between tholeiitic basalts and gabbros, representing oceanic crust or oceanic shelves to a bimodal calc-alkaline arc volcanism related to subduction.

6. Conclusion

The geological study carried out in the Alépé area gives an overall idea of the distribution of rocks and geological structures in the area studied. Thus, two lithological groups have been highlighted. The first is the volcanic magmatic set (amphibolite) and the second is the plutonic magmatic set (amphibole metagranite) to which are added the deposits of the continental terminal. The geochemical characterization confirms well this petrographic study and shows that the formations are of peraluminous to metaluminous types. These formations are of mantle origin but contain a certain crustal component, and their emplacement occurred in a collisional tectonic environment.

Conflicts of Interest

The authors declare no conflicts of interest regarding the publication of this paper.

References

[1] Bessoles, B. (1977) Geology of Africa, 1. West African Craton. Mém. B.R.G.M., Paris, No. 88, 404 p.

[2] Yacé, I. (1984) Le précambrien de l'Afrique de l'Ouest et ses corrélations avec le Brésil Oriental. Rapport Final. Publication IGCP-CIFEG, No. 2. Paris, 28.

[3] Zanone, L. (1964) The Manganese of the Ivory Coast. Rapport Multigr. SODEMI. N˚44 et 44 bis, 273.

[4] Sonnendrucker, P. (1968) Synthesis Study on the Gold of Ivory Coast. The Dispersed Gold-Bearing Regions. Rap. SODEMI. n˚220, 97 p.

[5] Delors, C., Diaby, I., Simeon, Y., Yao, B., Tastet, J., Vidal, M., Chiron, J.-C. and Dommanget, A. (1992) Explanatory Note of the Geological Map of Ivory Coast at 1/200000. Feuille de Grand-Bassam, Mémoire de la Direction de la géologie, n˚4, Abidjan, 9-15.

[6] Papon, A. (1973) Geology and Mineralization of South-West Côte d'Ivoire. Mémoire du BRGM, vol. 80, 284.

[7] Adingra, M.P.K. (2020) Petrostructural and Geochemical Characterization of the Birimian Formations of the South-Eastern Part of the Comoé Basin (North of Alépé—Southeast of Ivory Coast): Implication on the Geodynamic Evolution. PhD, Univ. Félix Houphouët Boigny, Boigny, 220. http://publication.lecames.org/index.php/svt/article/download/1450/827

[8] Vidal, M., Gumiaux, C., Cagnard, F., Pouclet, A., Ouattara, G. and Pichon, M. (2009) Evolution of a Paleoproterozoic "Weak Type" Orogeny in the West African

Craton (Ivory Coast). *Tectonophysics*, **477**, 145-159.
https://hal-insu.archives-ouvertes.fr/insu-00360070
https://doi.org/10.1016/j.tecto.2009.02.010

[9] Caby, R., Delor, C. and Agoh, O. (2000) Lithology, Structure and Metamorphism of the Birimian Formations in the Odienne Area [Ivory Coast]: The Major Role Played by Plutonic Diapirism and Strike-Slip Faulting at the Border of the Man Craton. *Journal of African Earth Sciences*, **30**, 351-374.
https://doi.org/10.1016/S0899-5362(00)00024-5

[10] Camil, J. (1984) Petrography, Chronology of the Archean Granulite Assemblages and Associated Formations of the Man Region (Ivory Coast). Thèse de doctorat, Univ. Abidjan, Abidjan, 306 p.

[11] Kouamelan, A.-N. (1996) Géochronologie et Géochimie des Formations Archéennes et Protérozoïques de la Dorsale de Man en Côte d'Ivoire. Implications pour la Transition Archéen-Protéozoïque. https://tel.archives-ouvertes.fr/tel-00653760

[12] Middlemost, E.A.K. (1994) Naming Materials in the Magma/Igneous Rock System. *Earth Science Reviews*, **37**, 215-224. https://doi.org/10.1016/0012-8252(94)90029-9

[13] De La Roche, H. (980) A Classification of Volcanic and Plutonic Rocks Using R1-R2 Diagram and Main—Analyzes His Current Relationship Nomenclature Item. *Chemical Geology*, **29**, 183-121. https://doi.org/10.1016/0009-2541(80)90020-0

[14] Pecerillo, R. and Taylor, S.R. (1976) Geochemistry of Eocene Calc-Alkaline Volcanic Rocks from the Kastamonu Area, Northern Turkey. *Contributions to Mineralogy and Petrology*, **58**, 63-81. https://doi.org/10.1007/BF00384745

[15] Irvine, T.N. and Baragar, W.R.A. (1971) A Guide to the Chemical Classification of the Common Volcanic Rocks. *Canadian Journal of Earth Sciences*, **8**, 523-548.
https://doi.org/10.1139/e71-055

[16] Shand, S.J. (1922) The Problem of the Alkaline Rocks. *Proceedings of the Geological Society of South Africa*, **25**, 19-33.

[17] Vidal, M. and Alric, G. (1994) The Paleoproterozoic (Birimian) of Haute-Comoé in the West African Craton, Ivory Coast: A Transtensional Back-Arc Basin. *Precambrian Research*, **65**, 207-229. https://doi.org/10.1016/0301-9268(94)90106-6

[18] Barbarin, B. and Didier, J. (1992) Genesis and Evolution of Mafic Microgranular Enclaves through Various Types of Interaction between Coexisting Felsic and Mafic Magmas. *Transactions of the Royal Society of Edinburgh*: *Earth Sciences*, **83**, 145-153.
https://doi.org/10.1017/S0263593300007835

[19] Adam, H. (1969) Report n˚255 of the End of the 1968-1969 Campaign Concerning the Regions of Aboisso-Comoé, Béttié, Kétesso, Bianouan, Apprompro-Zaranou, Alosso, SODEMI, pp 5-41. Adam H. Rapport n˚260 de fin de campagne 1969-1970 de la mission du Sud-Est, SODEMI, 38.

[20] Letalenet, J. (1962) Rapport sur la prospection des granites du Sud-Est de la Côte d'Ivoire (région d'Agboville). Rapport BRGM, 47 multigr., Abidjan.

[21] Teha, K.R., Kouamelan, A.N., Allialy, M.E., Djro, S.C., Houssou, N.N., Koffi, Y.A., Pria, K., Kossonou, J.M., Kouassi, B.R. and Koffi, G.S. (2018) Petrographic and Geochemical Character of Birimian Granitoids from the Comoé Basin and Surrounding Area (Southern Côte d'Ivoire). *International Journal of Engineering Science Invention*, **7**, 16-25.
http://www.ijesi.org/papers/Vol(7)i12/Version-3/C0712031625.pdf

[22] Bard, J.-P. (1975) Classification and Origin of the Eburnian Granitoids of the West African Craton. *Comptes Rendus de l Académie des Sciences*, **278**, 867-870.

[23] Yacé, I. (1976) Le volcanisme éburnéen dans les parties centrales et méridionales de

la chaîne précambrienne de Fettekro en Côte d'Ivoire. Thèse d'Etat, ès Sci. Université d'Abidjan, Abidjan, 376-13 f.

[24] Houssou, N. (2013) Petrological, Structural and Metallogenic Study of the Agbahou Gold Deposit, Divo, Ivory Coast. PhD Thesis, Université Felix Houphouët-Boigny, Boigny, 257.

[25] Tagini, B. (1971) Esquisse structurale de la Côte d'Ivoire. Essai de géotectonique régionale. Thèse de doctorat Fac. Sci. Univ. Lausanne. Rapp. SODEMI, Abidjan, 266.

[26] Vidal, M., Delor, C., Pouclet, A., Simeon, Y. and Alric, G. (1996) Geodynamic Evolution of West Africa between 2.2 Ga and 2 Ga: The "Archean" Style of the Green Belts and Birimian Sedimentary Assemblages of Northeastern Côte d'Ivoire. *Bulletin de la Société Géologique de France*, **167**, 307-319.

[27] Guibert, Ph. and Vidal, M. (1984) A Model of Structural Evolution of the Birimian of Southeastern Côte d'Ivoire. *Anna University Abidjan*, *Series C* (*Sciences*), **20**, 277-293.

[28] Gasquet, D., Barbey, P., Adou, M. and Paquette, J.L. (2003) Structure Sr-Nd Isotope Geochemistry and Zircon U-Pb Geochronology of the Granitoids of the Dabakala Area (Côte d'Ivoire): Evidence for a 2.3 Ga Crustal Growth Event in the Palaeoproterozoic of West Africa? *Precambrian Research*, **127**, 329-354. https://doi.org/10.1016/S0301-9268(03)00209-2

[29] Gnanzou, A. (2014) Study of the Volcano-Sedimentary Series of the Dabakala Region (North-East Ivory Coast): Genesis and Magmatic Evolution. Contribution to the Knowledge of the Bobosso Gold Mineralization in the Haute-Comoé Series. PhD, Univ. Paris-Sud Orsay, France and Univ. Félix Houphouët, Boigny, 303. https://theses.hal.science/tel-01127955/document

[30] Abouchami, W., Boher, M., Michard, A. and Albare de, F. (1990) A Major 2.1 Ga Event of Mafic Magmatism in West Africa: An Early Stage of Crustal Accretion. *Journal of Geophysical Research*, **95**, 17605-17629. https://doi.org/10.1029/JB095iB11p17605

[31] McLennan, S.M., Hemming, S., Taylor, S.R. and Eriksson, K.A. (1995) Early Proterozoic Crustal Evolution: Geochemical and Nd-Pb Isotopic Evidence from Metasedimentary Rocks Southwestern North America. *Geochimica et Cosmochimica Acta*, **59**, 1153-1173. https://doi.org/10.1016/0016-7037(95)00032-U

[32] Pearce, J.A. and Cann, J.R. (1973) Tectonic Setting of Basic Volcanic Rocks Determined Using Trace Element Analyses. *Earth and Planetary Science Letters*, **19**, 290-300. https://doi.org/10.1016/0012-821X(73)90129-5

[33] Bonnot-Courtois, C. (1981) Géochimie des Terres Rares dans les principaux milieux de formation et de sédimentation des argiles. Thèse, Université Paris Sud Centre d'Orsay, Paris, 251.